International Journal of Research in Engineering and Science (IJRES)
ISSN (Online): 2320-9364, ISSN (Print): 2320-9356
www.ijres.org Volume 5 Issue 10 ǁ October. 2017 ǁ PP. 41-49

Dissociative Excitation of the odd Quartet Levels of Cobalt Atom in e–$CoCl_2$ Collisions

*Smirnov Yu.M.
(Department of Physics-1, National Research University «MPEI», Moscow, Russia)
*Corresponding Author: *Smirnov Yu.M.*

ABSTRACT: *The method of extended crossing beams accompanied with optical signal recording was used to study inelastic collisions of slow electrons with cobalt dichloride molecules leading to formation of excited cobalt atoms in odd quartet states. Eighty-four cross-sections arising owing to dissociative excitation of CoI spectral lines have been measured at an exciting electron energy of 100 eV. Eight optical excitation functions (OEFs) have been recorded with incident electron energies varying between 0 and 100 eV. These findings have been used to compute of excitation cross-sections for the cobalt atom energy levels and the contribution of cascade transitions into their population. A comparison of excitation cross-sections for e–Co vs. e–$CoCl_2$ is presented.*

Keywords: *extended crossing beams, dissociative excitation, cross-section, spectral line, energy level*

Date of Submission: 17-05-2017 Date of acceptance: 27-10-2017

I. INTRODUCTION

The formation of excited particles (atoms, ions, molecules, radicals) in multi-component low-temperature plasma affects the velocity of various plasma-chemical reactions substantially [1]. While some molecules may become excited without chemical bonds breaking down, a major part is played processes that involve dissociation of molecules giving rise to excited dissociation products (dissociative excitation). While multi-stage particle excitation processes are predominant in relatively dense plasmas, it is not the case with low-density plasmas and beam plasmas where dissociative excitation is the result of one-off collisions between electrons and original molecules. In particular, this is the situation faced by designers of high-power selective UV radiation sources: "Essentially, the design of selective (narrow-band) UV radiation sources has to rely on three pathways for energy contributing to the medium: excitation with a high-energy electron beam, electric discharge within the radiating medium and heavy-particle pumping of gaseous media of various compositions (or any combination of the three)…" [2].

Despite the potentially significant role that dissociative collisions may play in the shaping plasma properties, they have only been afforded scant theoretical consideration so far. The author was only successful in discovering two theoretical papers addressing the dissociative excitation process. The study [3] is concerned with generation of oxygen atoms in a high-lying metastable state $2p^3 3s\ ^5S^\circ_2$ upon collisions of electrons with oxygen molecules. A later fundamental study [4] examines the dependence of dissociative excitation cross-sections upon the vibrational quantum number of the initial state for hydrogen and deuterium molecules. Electron collisions with vibrationally excited H_2 and D_2 molecules have been considered giving rise to paired atoms, one in the ground state 1*s* and the other in the excited state 2*p*. It should be noted that [3, 4] are concerned with homoatomic molecules. No similar studies of any heteroatomic molecules have been published so far.

In contrast, extensive findings are available from experimental studies of dissociative excitation. Most experimental setups featured extended electron beams. Gas-filled cell mode was used for studies of homoatomic hydrogen [5], oxygen [6], nitrogen [7] molecules while the crossing beam mode was used in experiments with Te_2 [8] and Se_2 [9]. All studies of electron collisions with oxide molecules (for example, YO [10]) and metal halides (for example, KI [11], $FeCl_2$ [12]) used the extended crossing electron and molecular beams.

Past studies of inelastic collisions of electrons with cobalt dichloride molecules have already yielded findings representing the dissociative excitation of the cobalt atom doublet levels [13]. This study provides information on dissociative excitation cross-sections of odd quartet levels of CoI.

Similar to previous studies the experiment relies on the method of extended crossing beams described in greater detail in [14, 15]. Key conditions of the particular experiment with $CoCl_2$ are summarized in [16]. Thus, it would be superfluous to duplicate the experimental technique and method in this paper.

II. RESULTS AND DISCUSSION

The optical emission spectrum resulting from inelastic collisions of cobalt dichloride molecules with a beam of monoenergetic electrons (E = 100 eV) has been recorded in the wavelength range λ = 280–570 nm. More than 200 spectrum lines have been discovered and identified as belonging to the CoI spectrum based on data from [17]. As reported in [18], this spectral range also features 12 systems of cobalt monochloride $^{59}Co^{35}Cl$ bands, however neither could be reliably discovered given the conditions of this study. For spectral lines of cobalt atom arising as a result of spontaneous transitions originating at odd quartet levels, eight optical excitation functions (OEFs) have been recorded within electron energy range of 0–100 eV in addition to dissociative excitation cross-sections measured at exciting electron energy of 100 eV. Findings complemented with requisite spectroscopic data are stated in Table 1 (transitions having OEFs recorded) and Table 2 (transitions for which adequately reliable recording of OEFs proved impossible). The tables indicate

Table 1 Dissociative Excitation Cross-Sections of Cobalt Atom (with OEFs recorded)

λ (nm)	Transition	J_{low}–J_{up}	E_{low} (cm^{-1})	E_{up} (cm^{-1})	Q_{100} (10^{-18} cm^2)	Q_{max} (10^{-18} cm^2)	$E(Q_{max})$ (eV)	*OEF*
340.918	$3d^8(^3F)4s\ b^4F–3d^8(^3F)4p\ y^4F°$	7/2–7/2	4142	33466	0.52	0.60;0.60	60;72	5
341.263	$3d^74s^2\ a^4F–3d^7(^4F)4s4p(^3P°)\ z^4D°$	9/2–7/2	0	29294	1.07	1.19	44	1
343.158	$3d^74s^2\ a^4F–3d^7(^4F)4s4p(^3P°)\ z^4D°$	7/2–5/2	816	29948	0.83	0.92	44	1
344.944	$3d^8(^3F)4s\ b^4F–3d^8(^3F)4p\ y^4G°$	9/2–9/2	3482	32464	0.24	0.32	62	7
345.351	$3d^8(^3F)4s\ b^4F–3d^8(^3F)4p\ y^4G°$	9/2–11/2	3482	32430	1.38	1.65	55	8
346.580	$3d^74s^2\ a^4F–3d^7(^4F)4s4p(^3P°)\ z^4G°$	9/2–11/2	0	28845	1.86	2.16	53	6
347.402	$3d^8(^3F)4sb^4F–3d^8(^3F)4py^4F°$	5/2–7/2	4690	33466	0.91	1.06	60;72	5
	$3d^74s^2\ a^4F–3d^7(^4F)4s4p(^3P°)\ z^4F°$	9/2–7/2	0	28777			53	3
350.263	$3d^74s^2\ a^4F–3d^7(^4F)4s4p(^3P°)\ z^4D°$	5/2–5/2	1406	29948	0.28	0.31	44	1
351.043	$3d^74s^2\ a^4F–3d^7(^4F)4s4p(^3P°)\ z^4D°$	7/2–7/2	816	29294	0.63	0.70	44	1
352.685	$3d^74s^2\ a^4F–3d^7(^4F)4s4p(^3P°)\ z^4F°$	9/2–9/2	0	28345	2.87	3.35	75	4
352.982	$3d^8(^3F)4s\ b^4F–3d^8(^3F)4p\ y^4G°$	7/2–9/2	4142	32464	0.88	1.17	62	7
355.059	$3d^74s^2\ a^4F–3d^7(^4F)4s4p(^3P°)\ z^4F°$	5/2–3/2	1406	29563	0.10	0.107	83	2
357.536	$3d^74s^2\ a^4F–3d^7(^4F)4s4p(^3P°)\ z^4F°$	7/2–7/2	816	28777	0.91	1.07	53	3
360.208	$3d^74s^2\ a^4F–3d^7(^4F)4s4p(^3P°)\ z^4F°$	3/2–3/2	1809	29563	0.32	0.34	83	2
363.139	$3d^74s^2\ a^4F–3d^7(^4F)4s4p(^3P°)\ z^4F°$	7/2–9/2	816	28345	0.17	0.20	75	4
365.254	$3d^74s^2\ a^4F–3d^7(^4F)4s4p(^3P°)\ z^4F°$	5/2–7/2	1406	28777	0.22	0.26	53	3
387.312	$3d^8(^3F)4s\ b^4F–3d^7(^4F)4s4p(^3P°)\ z^4D°$	9/2–7/2	3482	29294	0.67	0.75	44	1
387.395	$3d^8(^3F)4s\ b^4F–3d^7(^4F)4s4p(^3P°)\ z^4D°$	7/2–5/2	4142	29948	0.49	0.54	44	1
394.173	$3d^8(^3F)4s\ b^4F–3d^7(^4F)4s4p(^3P°)\ z^4G°$	9/2–11/2	3482	28845	0.13	0.15	53	6
395.793	$3d^8(^3F)4s\ b^4F–3d^7(^4F)4s4p(^3P°)\ z^4D°$	5/2–5/2	4690	29948	0.090	0.10	44	1
397.473	$3d^8(^3F)4s\ b^4F–3d^7(^4F)4s4p(^3P°)\ z^4D°$	7/2–7/2	4142	29294	0.13	0.145	44	1
399.531	$3d^8(^3F)4s\ a^2F–3d^8(^3F)4p\ y^4G°$	7/2–9/2	7442	32464	0.59	0.79	62	7
402.090	$3d^8(^3F)4s\ b^4F–3d^7(^4F)4s4p(^3P°)\ z^4F°$	9/2–9/2	3482	28345	0.22	0.26	75	4
405.818	$3d^8(^3F)4s\ b^4F–3d^7(^4F)4s4p(^3P°)\ z^4F°$	7/2–7/2	4142	28777	0.16	0.19	53	3
415.043	$3d^8(^3F)4s\ b^4F–3d^7(^4F)4s4p(^3P°)\ z^4F°$	5/2–7/2	4690	28777	0.065	0.077	53	3
444.195	$3d^8(^3F)4s\ a^2F–3d^7(^4F)4s4p(^3P°)\ z^4D°$	7/2–5/2	7442	29948	0.091	0.10	44	1
468.586	$3d^8(^3F)4s\ a^2F–3d^7(^4F)4s4p(^3P°)\ z^4F°$	7/2–7/2	7442	28777	0.21	0.25	53	3

Table 2 Dissociative Excitation Cross-Sections of Cobalt Atom (without OEFs recorded)

λ (nm)	Transition	J_{low}–J_{up}	E_{low} (cm^{-1})	E_{up} (cm^{-1})	Q_{100} (10^{-18} cm^2)
1	2	3	4	5	6
280.377	$3d^8(^3F)4s\ b^4F–3d^7(^4F)4s4p(^1P°)\ x^4D°$	5/2–5/2	4690	40345	0.30
281.151	$3d^8(^3P)4s\ b^4P–3d^8(^3F)5p\ s^4D°$	5/2–7/2	15184	50741	0.36
282.680	$3d^8(^3P)4s\ b^4P–3d^8(^3F)5p\ s^4D°$	3/2–5/2	15774	51139	0.24
283.443	$3d^8(^3F)4s\ b^4F–3d^7(^4F)4s4p(^1P°)\ x^4D°$	3/2–5/2	5075	40345	0.14
297.801	$3d^8(^3P)4s\ b^4P–3d^7(^2P)4s4p(^3P°)\ x^4S°$	5/2–3/2	15184	48753	0.18
340.512	$3d^8(^3F)4s\ b^4F–3d^8(^3F)4p\ y^4F°$	9/2–9/2	3482	32841	1.60
341.715	$3d^8(^3F)4s\ b^4F–3d^8(^3F)4p\ y^4F°$	5/2–5/2	4690	33945	0.39
343.305	$3d^8(^3F)4s\ b^4F–3d^8(^3F)4p\ y^4F°$	3/2–3/2	5075	34196	0.56
344.292	$3d^74s^2\ a^4F–3d^7(^4F)4s4p(^3P°)\ z^4D°$	5/2–3/2	1406	30443	0.55
344.364	$3d^8(^3F)4s\ b^4F–3d^8(^3F)4p\ y^4G°$	7/2–7/2	4142	33173	0.68
344.917	$3d^8(^3F)4s\ b^4F–3d^8(^3F)4p\ y^4G°$	5/2–5/2	4690	33674	0.31
345.524	$3d^74s^2\ a^4F–3d^7(^4F)4s4p(^3P°)\ z^4D°$	3/2–1/2	1809	30742	0.34
346.280	$3d^8(^3F)4s\ b^4F–3d^8(^3F)4p\ y^4F°$	3/2–5/2	5075	33945	0.67
349.132	$3d^74s^2\ a^4F–3d^7(^4F)4s4p(^3P°)\ z^4D°$	3/2–3/2	1809	30443	0.15
349.568	$3d^8(^3F)4s\ b^4F–3d^8(^3F)4p\ y^4G°$	3/2–5/2	5075	33674	0.185
350.228	$3d^8(^3F)4s\ b^4F–3d^8(^3F)4p\ y^4D°$	9/2–7/2	3482	32027	1.36

1	2	3	4	5	6
350.631	$3d^8(^3F)4s\ b^4F–3d^8(^3F)4p\ y^4D°$	7/2–5/2	4142	32654	0.57
350.984	$3d^8(^3F)4s\ b^4F–3d^8(^3F)4p\ y^4G°$	5/2–7/2	4690	33173	0.23
351.264	$3d^8(^3F)4s\ b^4F–3d^8(^3F)4p\ y^4D°$	5/2–3/2	4690	33150	0.37
351.348	$3d^74s^2\ a^4F–3d^7(^4F)4s4p(^3P°)\ z^4G°$	7/2–9/2	816	29269	1.18
352.007	$3d^74s^2\ a^4F–3d^7(^4F)4s4p(^3P°)\ z^4F°$	7/2–5/2	816	29216	0.15
352.342	$3d^8(^3F)4s\ b^4F–3d^8(^3F)4p\ y^4D°$	3/2–1/2	5075	33449	0.155
352.903	$3d^74s^2\ a^4F–3d^7(^4F)4s4p(^3P°)\ z^4G°$	5/2–7/2	1406	29735	0.82
353.336	$3d^74s^2\ a^4F–3d^7(^4F)4s4p(^3P°)\ z^4G°$	3/2–5/2	1809	30102	0.58
354.671	$3d^74s^2\ a^4P–3d^8(^3P)4p\ z^4P°$	5/2–3/2	13795	41982	0.105
354.844	$3d^74s^2\ a^4P–3d^8(^3P)4p\ z^4P°$	5/2–5/2	13795	41968	0.43
356.089	$3d^8(^3F)4s\ b^4F–3d^8(^3F)4p\ y^4D°$	3/2–3/2	5075	33150	0.105
357.497	$3d^8(^3F)4s\ b^4F–3d^8(^3F)4p\ y^4D°$	5/2–5/2	4690	32654	0.21
357.890	$3d^74s^2a^4P–3d^8(^3P)4pz^4P°$	3/2–1/2	14036	41969	} 0.125
357.903	$3d^74s^2\ a^4P–3d^8(^3P)4p\ z^4P°$	3/2–5/2	14036	41968	
358.515	$3d^8(^3F)4s\ b^4F–3d^8(^3F)4p\ y^4D°$	7/2–7/2	4142	32027	0.14
359.487	$3d^74s^2\ a^4F–3d^7(^4F)4s4p(^3P°)\ z^4F°$	5/2–5/2	1406	29216	0.58
372.665	$3d^74s^2\ a^4P–3d^7(^4P)4s4p(^3P°)\ z^4S°$	5/2–3/2	13795	40621	0.081
373.048	$3d^8(^3P)4s\ b^4P–3d^8(^3P)4p\ z^4P°$	5/2–3/2	15184	41982	0.14
373.239	$3d^8(^3P)4s\ b^4P–3d^8(^3P)4p\ z^4P°$	5/2–5/2	15184	41968	0.19
376.040	$3d^74s^2\ a^4P–3d^7(^4P)4s4p(^3P°)\ z^4S°$	3/2–3/2	14036	40621	0.091
380.810	$3d^8(^3F)4s\ b^4F–3d^7(^4F)4s4p(^3P°)\ z^4G°$	9/2–7/2	3482	29735	0.13
381.632	$3d^8(^3P)4sb^4P–3d^8(^3P)4pz^4P°$	3/2–1/2	15774	41970	} 0.14
381.646	$3d^8(^3P)4s\ b^4P–3d^8(^3P)4p\ z^4P°$	3/2–5/2	15774	41969	
387.683 {	$3d^8(^3P)4sb^4P–3d^8(^3P)4pz^4P°$	1/2–3/2	16195	41982	} 0.21
	$3d^8(^3F)4s\ b^4F–3d^7(^4F)4s4p(^3P°)\ z^4G°$	9/2–9/2	3482	29269	
388.187	$3d^8(^3F)4s\ b^4F–3d^7(^4F)4s4p(^3P°)\ z^4D°$	5/2–3/2	4690	30443	0.35
389.498	$3d^8(^3F)4s\ b^4F–3d^7(^4F)4s4p(^3P°)\ z^4D°$	3/2–1/2	5075	30742	0.25
393.392	$3d^8(^3F)4s\ b^4F–3d^7(^4F)4s4p(^3P°)\ z^4G°$	5/2–5/2	4690	30102	0.074
393.596	$3d^8(^3F)4s\ a^2F–3d^8(^3F)4p\ y^4F°$	7/2–9/2	7442	32841	0.18
394.089	$3d^8(^3F)4s\ b^4F–3d^7(^4F)4s4p(^3P°)\ z^4D°$	3/2–3/2	5075	30443	0.10
398.712	$3d^8(^3F)4s\ b^4F–3d^7(^4F)4s4p(^3P°)\ z^4F°$	7/2–5/2	4142	29216	0.082
399.168	$3d^8(^3F)4s\ b^4F–3d^7(^4F)4s4p(^3P°)\ z^4G°$	5/2–7/2	4690	29735	0.15
399.454	$3d^8(^3F)4s\ b^4F–3d^7(^4F)4s4p(^3P°)\ z^4G°$	3/2–5/2	5075	30102	0.10
401.394	$3d^8(^3P)4s\ b^4P–3d^7(^4F)4s4p(^1P°)\ x^4D°$	1/2–1/2	16195	41101	0.18
402.340	$3d^8(^3P)4s\ b^4P–3d^7(^4P)4s4p(^3P°)z^4S°$	3/2–3/2	15774	40621	0.071
404.539	$3d^8(^3F)4s\ a^2F–3d^8(^3F)4p\ y^4G°$	5/2–7/2	8460	33173	0.044
405.860	$3d^8(^3P)4s\ b^4P–3d^7(^4F)4s4p(^1P°)\ x^4D°$	1/2–3/2	16195	40827	0.17
406.637	$3d^8(^3F)4s\ a^2F–3d^8(^3F)4p\ y^4D°$	7/2–7/2	7442	32027	0.051
406.854	$3d^8(^3P)4s\ b^4P–3d^7(^4F)4s4p(^1P°)\ x^4D°$	3/2–5/2	15774	40345	0.28
408.630	$3d^8(^3P)4s\ b^4P–3d^7(^4F)4s4p(^1P°)\ x^4D°$	5/2–7/2	15184	39649	0.36
448.671	$3d^74s^2\ b^2D–3d^7(^2G)4s4p(^3P°)\ w^4F°$	5/2–5/2	21920	44201	0.16
455.912	$3d^74s^2\ b^2D–3d^7(^2G)4s4p(^3P°)\ w^4F°$	5/2–7/2	21920	43847	0.27
467.092	$3d^74s^2\ b^2D–3d^7(^2G)4s4p(^3P°)\ w^4F°$	3/2–3/2	23152	44555	0.125
524.792	$3d^74s^2\ a^4P–3d^8(^3F)4p\ y^4D°$	1/2–1/2	14399	33449	0.12

wavelengths λ, transitions, full-momentum quantum numbers of the lower J_{low} and upper J_{up} levels, energies of the lower E_{low} and upper E_{up} levels (counted from the ground level of the cobalt atom), dissociative excitation cross-sections at exciting electron energy of 100 eV Q_{100} and at OEF maximum $Q_{\max}$, and the position of the maximum $E(Q_{\max})$. Reference data on spectroscopic properties of the transitions are cited per [17]. The last column of Table 1 indicates OEF numbers in accordance to their numbering on Fig. 1. Each curve has been assigned an individual zero reading level along the vertical axis. Curves have been positioned in a manner as to avoid any crossings or tangencies. All curves have been normalized to unity at their maxima.

Fig. 1 shows the shape of recorded OEFs to be typical for OEFs expected at dissociative excitation. They feature a complex structure in addition to the main maximum being rather remote from the threshold energy. In the low electron energy range (~ tens of eV), the following reactions are possible that may give rise to excited cobalt atoms:

$CoCl_2 + e \rightarrow Co^* + Cl_2 + e'$ (8.85), (1)

$\rightarrow Co^* + 2Cl + e'$ (11.35), (2)

$\rightarrow Co^* + Cl_2^* + e'$ (~11.4), (3)

$\rightarrow Co^* + Cl_2^+ + e' + e''$ (20.33), (4)

$\rightarrow Co^* + Cl + Cl^* + e'$ (~20.6), (5)

$\rightarrow Co^* + Cl + Cl^+ + e' + e''$ (24.32). (6)

Here, e and e' are incident and scattered electrons, respectively, and e'' is the electron knocked out of the chlorine atom or molecule upon their ionization. Asterisks denote excited particles. Values in parentheses next to reaction equations comprise computed values of minimal appearance energies E_{ap} in eV estimated for the spectral line λ = 352.685 nanometers. This line has the greatest excitation cross-section out of all values

measured in this paper and its OEF has been determined with the least error. Detailed discussion of the E_{ap} calculation and information source about the rupture of a chemical bonds in $CoCl_2$ molecule is given in [19].

An experimental reading of E_{ap} = 8.7 eV is consistent with the computed value for the reaction pathway (1). A similar result had been obtained in the past for odd doublet levels of CoI in [13]. The OEF produces its first local peak at incident electron energy of 9.8 eV, reaching a magnitude of ~17% of the cross-section value at the main maximum. After a minor depression, OEF resumes its ascent at E ~ 11.2 eV until it reaches a magnitude of ~38%; this peak is associated with reactions (2) and (3), of these two the reaction (3) can be viewed as the more likely cause. OEF makes its next upward turn at E ~ 20 eV; reactions (4) and (5) being the cause for the rise, and so on. As energy increases further, the number of potential competing pathways grows dramatically and the precision of E_{ap} computations drops.

Fig. 2 shows a partial energy-state diagram for the cobalt atom with the transitions under study. To make the plot more simple, terms have been plotted with blocks without *J*-split. Vertical dashed lines separate even and odd states. Sets of quantum state properties (configurations and terms) are placed below the horizontal axis in most cases. For even levels belonging to $3d^8(^3F)4s$ and $3d^7 4s^2$ configurations, terms have been indicated

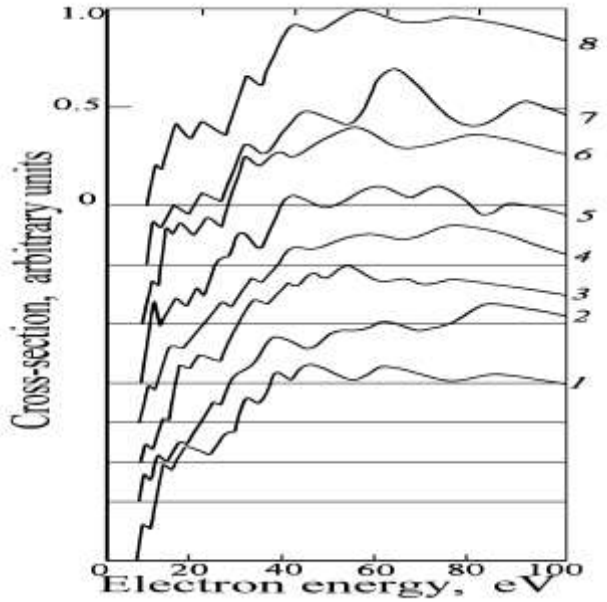

Fig. 1 Optical dissociative excitation functions of CoI

within the plot area, to the next of the respective blocks. For the transitions under study shown in Fig. 2, a considerable majority can be seen to occur within the limits of the quartet term system. Nevertheless, intercombination transitions ending at $3d^8(^3F)4s\ a^2F$ and $3d^7 4s^2\ b^2D$ have also been recorded.

In experiments based on recording spontaneous radiation by excited particles, excitation cross-sections Q_{ki} are measured for spectral lines corresponding to transition from the level k to the level i. However it is the excitation cross-sections q_k of energy levels that are the primary collision property relevant for theoretical treatment as well as a majority of practical applications. Values of q_k can be inferred from experimental findings using the relation:

$$q_k = \sum_i Q_{ki} - \sum_l Q_{lk} \ , \qquad (7)$$

where the left-hand sum take into consideration a competition between spontaneous transitions from the level k to all underlying levels i (branching) and the right-hand sum accounts for the contribution of cascade transitions to the all underlying levels i (branching) and the right-hand sum accounts for the contribution of cascade transitions to the level k originating at all overlying levels l.

The extent to which the relation (7) can account for the multitude of potential transitions is determined by two factors: 1) instrument sensitivity i.e. the likelihood of discovering weak lines, and 2) the practical spectral range of instruments i.e. whether it is possible to record spectral lines located in vacuum UV and IR parts of the spectrum. This gradation in case of factor 2) owes itself to the fact that studies of vacuum UV and IR ranges usually call for special instruments different from those used in visible-light and UV ranges (i.e. vacuum monochromators and IR spectrometers).

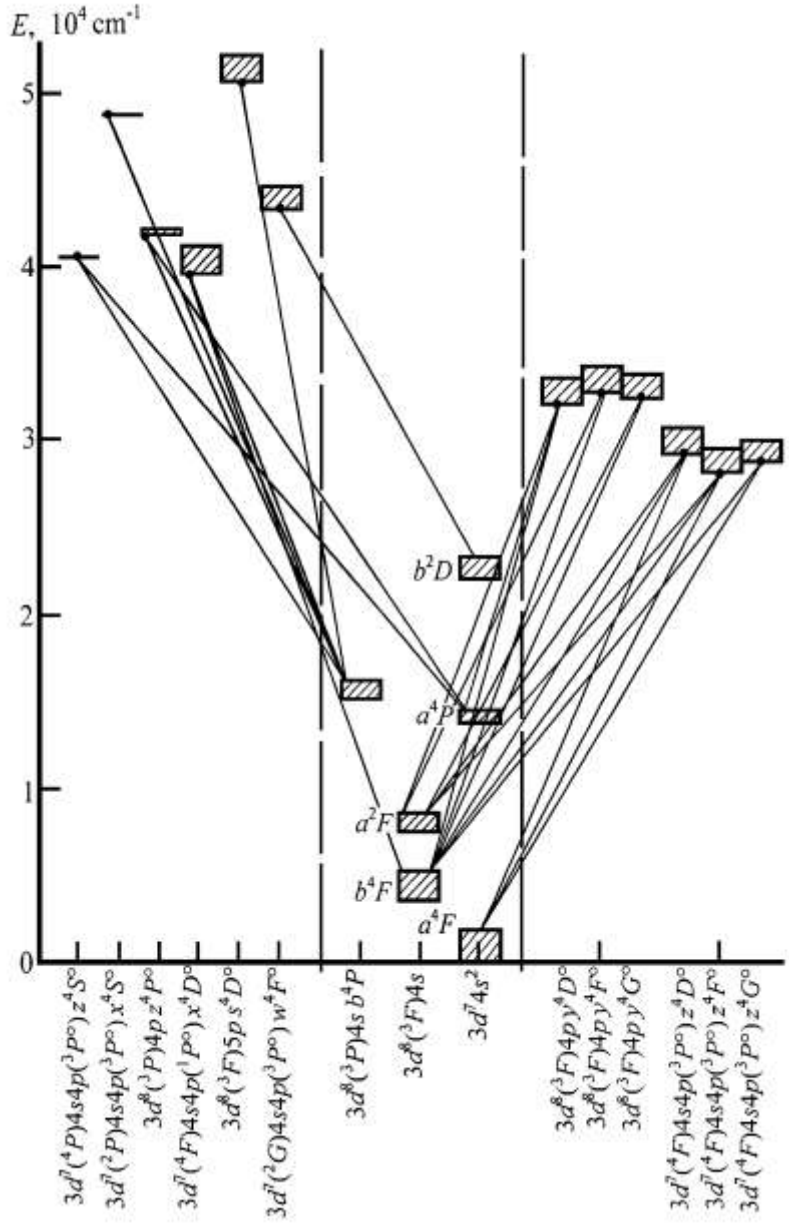

Fig. 2 Partial energy-state diagram for the cobalt atom with the transitions under study

Computations based on our findings presented in Tables 1, 2 have yielded dissociative excitation cross-section values at excitation electron energy of 100 eV, $\Sigma Q_{100} \equiv \sum_i Q_{ki}$, the contribution of cascade transitions $\Sigma Q' \equiv \sum_l Q_{lk}$, direct excitation cross-sections of levels q_k as well as the percent-wise contribution of cascade population $\Sigma Q'/\Sigma Q_{100}$ in the full excitation cross-sections of energy levels. Computed values are presented in Table 3; in the lines denoted with the Σ symbol presented properties for each term summarized by *J*. It can now be seen from Table 3 that cascade population contribution found in 18–30% range for four levels (three of these being $z^4D°_J$), for 20 levels the contribution by cascade population exceeds 30%, rising beyond 50% for 13 levels. There are three instances where $\Sigma Q'/\Sigma Q_{100} > 100\%$ as our data on branching from these levels is incomplete.

Findings from the measurement of dissociative excitation cross-sections in e–$CoCl_2$ collisions can be compared with direct excitation cross-sections for the respective transitions in e–Co electron-atom collisions. Such a comparison would characterize the effect the chemical bond between atoms in the molecule has on cross-section values. Direct excitation cross-sections have been measured by the author for the cobalt atom as a part of

a study program concerned with inelastic electron-atom collisions. For odd quartet levels, the respective values have been partially published in [20, 21].

Table 3 Dissociative Excitation Cross-Sections of CoI Energy Levels and Cascade Contribution

Configuration	Term	J	E_{up} (cm^{-1})	ΣQ_{100} (10^{-18} cm^2)	$\Sigma Q'$ (10^{-18} cm^2)	q_k (10^{-18} cm^2)	$\Sigma Q'/\Sigma Q_{100}$ %
$3d^7(^4P)4s4p(^3P°)$	$z^4S°$	3/2	40621	0.24			
$3d^7(^2P)4s4p(^3P°)$	$x^4S°$	3/2	48753	0.18			
$3d^8(^3P)4p$	$z^4P°$	1/2	41969	0.075			
		3/2	41982	0.30			
		5/2	41968	0.81			
		Σ		1.185			
$3d^7(^4F)4s4p(^3P°)$	$z^4D°$	1/2	30742	0.59	0.24	0.35	40.7
		3/2	30443	1.15	0.30	0.85	26.1
		5/2	29948	1.78	0.51	1.27	28.7
		7/2	29294	2.50	0.58	1.92	23.2
		Σ		6.02	1.63	4.39	27.1
$3d^8(^3F)4p$	$y^4D°$	1/2	33449	0.275	0.145	0.13	52.7
		3/2	33150	0.475	0.265	0.21	55.8
		5/2	32654	0.78	0.81	(-0.03)	104.
		7/2	32027	1.55	0.68	0.87	43.9
		Σ		3.08	1.90	1.18	61.7
$3d^7(^4F)4s4p(^1P°)$	$x^4D°$	1/2	41101	0.18			
		3/2	40827	0.17			
		5/2	40345	0.72			
		7/2	39649	0.36			
		Σ		1.43			
$3d^7(^4F)4s4p(^3P°)$	$z^4F°$	3/2	29563	0.42	0.59	(-0.17)	141.
		5/2	29216	0.81	0.27	0.54	33.3
		7/2	28777	1.56	2.00	(-0.44)	128.
		9/2	28345	3.26	0.60	2.66	18.4
		Σ		6.05	3.46	2.59	57.2
$3d^8(^3F)4p$	$y^4F°$	3/2	34196	0.56	0.50	0.06	89.3
		5/2	33945	1.06	0.71	0.35	67.0
		7/2	33466	1.23	0.38	0.85	30.9
		9/2	32841	1.78	1.47	0.31	82.6
		Σ		4.63	3.06	1.57	66.1
$3d^7(^2G)4s4p(^3P°)$	$w^4F°$	3/2	44555	0.125			
		5/2	44201	0.16			
		7/2	43847	0.27			
		Σ		0.555			
$3d^7(^4F)4s4p(^3P°)$	$z^4G°$	5/2	30102	0.75	0.23	0.52	30.7
		7/2	29735	1.10	0.51	0.59	46.4
		9/2	29269	1.33	0.80	0.53	60.1
		11/2	28845	1.99	0.87	1.12	43.7
		Σ		5.17	2.41	2.76	46.7
$3d^8(^3F)4p$	$y^4G°$	5/2	33674	0.49	0.305	0.185	62.2
		7/2	33173	0.95	0.49	0.46	51.6
		9/2	32464	1.71	1.24	0.47	72.5
		11/2	32430	1.38	1.07	0.31	77.5
		Σ		4.53	3.105	1.425	68.5
$3d^7(^2H)4s4p(^3P°)$	$^4H°$	9/2	50902	0.59			
		11/2	50703	0.155			
		Σ		0.745			

Table 4 summarizes the findings from comparison the values of dissociative excitation cross-sections in electron-molecule collisions with incident electron energy of 100 eV $Q_m(100)$ against direct excitation cross-section values in electron-atom collisions at incident electron energy of 50 eV $Q_a(50)$. Asterisks denote cross-section values that belong to unresolved by our apparatus spectral lines. It follows from findings presented in Table 4 that dissociative excitation is more efficient than direct excitation for terms $3d^7(^4P)4s4p(^3P°)$ $z^4S°_{3/2}$, $3d^8(^3P)4p(^3P°)$ $z^4P°$, $3d^7(^4F)4s4p(^1P°)$ $x^4D°$, $3d^7(^2G)4s4p(^3P°)$ $w^4F°$. All these terms are located at $E > 40000$ cm^{-1} and have comparatively small direct excitation cross-sections. For the rest of the terms studied, the value Q_a/Q_m is significantly above unity. The empirical regularities identified by us lack any theoretical interpretation so far, as there were few theoretical researches into regularities of dissociative excitation.

Table 4 summarizes the findings from comparison the values of dissociative excitation cross-sections in electron-molecule collisions with incident electron energy of 100 eV $Q_m(100)$ against direct excitation cross-section values in electron-atom collisions at incident electron energy of 50 eV $Q_a(50)$. Asterisks denote cross-

section values that belong to unresolved by our apparatus spectral lines. It follows from findings presented in Table 4 that dissociative excitation is more efficient than direct excitation for terms $3d^7(^4P)4s4p(^3P°)\ z^4S°_{3/2}$, $3d^8(^3P)4p(^3P°)\ z^4P°$, $3d^7(^4F)4s4p(^1P°)\ x^4D°$, $3d^7(^2G)4s4p(^3P°)\ w^4F°$. All these terms are located at E>40000 cm^{-1}

Table 4 Comparison of Excitation Cross-Sections of Cobalt Atom in Collisions e–Co and e–$CoCl_2$

λ (nm)	Upper Level	E (cm^{-1})	$Q_m(100)$ (10^{-18} cm^2)	$Q_a(50)$ (10^{-18} cm^2)	Q_a/Q_m
372.665	$3d^7(^4P)4s4p(^3P°)\ z^4S°_{3/2}$	40621	0.081	0.057	0.704
402.340			0.071	0.052	0.732
381.632	$3d^8(^3P)4p\ z^4P°_{1/2}$	41969	0.14*	0.089*	0.635
373.048	$3d^8(^3P)4p\ z^4P°_{3/2}$	41982	0.14	0.049	0.350
387.683			0.15*	0.050*	0.333
354.844	$3d^8(^3P)4p\ z^4P°_{5/2}$	41968	0.43	0.10	0.232
373.239			0.19	0.094	0.494
381.646			0.14*	0.089*	0.635
345.524	$3d^7(^4F)4s4p(^3P°)\ z^4D°_{1/2}$	30742	0.34	0.30	0.883
389.498			0.25	0.26	1.04
344.292	$3d^7(^4F)4s4p(^3P°)\ z^4D°_{3/2}$	30443	0.55	1.46	2.66
349.132			0.15	0.28	1.87
388.187			0.35	0.67	1.91
394.089			0.10	0.21	2.10
343.158	$3d^7(^4F)4s4p(^3P°)\ z^4D°_{5/2}$	29948	0.83	2.22	2.67
350.263			0.28	0.74	2.64
387.395			1.16*	2.06	1.78
395.793			0.090	0.15	1.67
341.263	$3d^7(^4F)4s4p(^3P°)\ z^4D°_{7/2}$	29294	1.07	5.86	5.48
351.043			0.63	1.72	2.73
387.312			1.16*	3.48	3.00
397.473			0.063	0.15	2.38
352.342	$3d^8(^3F)4p\ y^4D°_{1/2}$	33449	0.155	0.70	4.52
351.264	$3d^8(^3F)4p\ y^4D°_{3/2}$	33150	0.37	1.92	5.19
356.089			0.105	0.46	4.38
350.631	$3d^8(^3F)4p\ y^4D°_{5/2}$	32654	0.57	2.54	4.46
357.497			0.21	0.73	3.47
350.228	$3d^8(^3F)4p\ y^4D°_{7/2}$	32027	1.36	5.30	3.90
358.515			0.14	0.48	3.43
406.637			0.051	0.18	3.54
401.394	$3d^7(^4F)4s4p(^1P°)\ x^4D°_{1/2}$	41101	0.18	0.078	0.433
280.377	$3d^7(^4F)4s4p(^1P°)\ x^4D°_{5/2}$	40345	0.30	0.28	0.935
406.854			0.28	0.34	1.21
408.630	$3d^7(^4F)4s4p(^1P°)\ x^4D°_{7/2}$	39649	0.36	1.44	4.00
281.151	$s^4D°_{7/2}$	50741	0.36	0.32	0.890
355.059	$3d^7(^4F)4s4p(^3P°)\ z^4F°_{3/2}$	29563	0.10	0.48	4.80
360.208			0.32	1.45	4.53
352.007	$3d^7(^4F)4s4p(^3P°)\ z^4F°_{5/2}$	29216	0.19	1.24	6.52
359.487			0.58	2.92	5.03
347.402	$3d^7(^4F)4s4p(^3P°)\ z^4F°_{7/2}$	28777	0.91*	6.12*	6.73
357.536			0.91	5.80	6.37
415.043			0.065	0.26	4.00
352.685	$3d^7(^4F)4s4p(^3P°)\ z^4F°_{9/2}$	28345	2.87	19.5	6.80
363.139			0.17	0.90	5.30
402.090			0.22	0.97	4.40
343.305	$3d^8(^3F)4p\ y^4F°_{3/2}$	34196	0.56	1.58	2.82
341.715	$3d^8(^3F)4p\ y^4F°_{5/2}$	33945	0.39	0.80	2.05
346.280			0.67	2.16	3.22
340.918	$3d^8(^3F)4p\ y^4F°_{7/2}$	33466	0.52	1.70	3.27
347.402			0.91*	6.12*	6.73
340.512	$3d^8(^3F)4p\ y^4F°_{9/2}$	32841	1.60	13.0	8.13
393.596			0.18	0.99	5.50
467.092	$3d^7(^2G)4s4p(^3P°)\ w^4F°_{3/2}$	44555	0.125	0.057	0.456
455.912	$3d^7(^2G)4s4p(^3P°)\ w^4F°_{7/2}$	43847	0.11	0.041	0.372
353.336	$3d^7(^4F)4s4p(^3P°)\ z^4G°_{5/2}$	30102	0.58	2.19	3.78
393.392			0.074	0.27	3.65
399.454			0.10	0.31	3.10
352.903	$3d^7(^4F)4s4p(^3P°)\ z^4G°_{7/2}$	29735	0.82	4.70	5.73
399.168			0.15	0.74	4.77
351.348	$3d^7(^4F)4s4p(^3P°)\ z^4G°_{9/2}$	29269	1.18	8.18	6.92
387.683			0.063*	0.38	6.05
346.580	$3d^7(^4F)4s4p(^3P°)\ z^4G°_{11/2}$	28845	1.86	19.1	10.2
394.173			0.13	0.99	7.63

344.917	$3d^8(^3F)4p\ y^4G°_{5/2}$	33674	0.31*	1.16	3.75
349.568			0.185	0.90	4.86
344.364	$3d^8(^3F)4p\ y^4G°_{7/2}$	33173	0.68	3.22	4.73
350.984			0.23*	1.04	4.52
404.539			0.044	0.15	3.41
344.944	$3d^8(^3F)4p\ y^4G°_{9/2}$	32464	0.24*	0.90	3.75
352.982			0.88	3.50	3.98
399.531			0.59	2.74	4.65
345.351	$3d^8(^3F)4p\ y^4G°_{11/2}$	32430	1.38	9.25	6.70

and have comparatively small direct excitation cross-sections. For the rest of the terms studied, the value Q_d/Q_m is significantly above unity. The empirical regularities identified by us lack any theoretical interpretation so far, as there were few theoretical researches into regularities of dissociative excitation.

III. CONCLUSION

A pioneering study was undertaken to obtain experimental data on dissociative excitation cross-sections for odd quartet levels of the cobalt atom in collisions between slow electrons and cobalt dichloride molecules. The resulting findings on excitation cross-sections for CoI spectral lines have been used to determine excitation cross-sections for energy levels and the contribution of cascade transitions to their population. When direct and dissociative excitation modes are compared against each other, it is revealed that dissociative excitation takes place more efficiently than does direct excitation in case of terms $z^4S°$, $z^4P°$, $x^4D°$, $w^4F°$. For the rest of terms studied, dissociative excitation cross-sections are several times less than their direct excitation analogy. The distribution of the molecule dissociation products over energy levels is of a great importance for the physics of multi-component low-temperature plasmas, as this distribution pattern can affect chemical reactivity of the plasma dramatically, shaping its optical properties as well.

REFERENCES

[1]. L. T. Bugaenko, M. G. Kuz'min, and L. S. Polak, Khimiya Vysokikh Energiy (High Energy Chemistry) (Moscow: Khimiya, 1988).

[2]. A. A. Al'okhin, V. A. Barinov, Yu. V. Geras'ko, O. F. Kostenko, F. N. Liubchenko, A. V. Tiukavkin, and V. I. Shalashkov, Nepreryvnye Plazmochmicheskiye Istochniki Sveta (Continuous Plasma-Chemical Light Source) (Moscow: BIOR, 1997. P. 5).

[3]. W. C. Wells, W. L. Borst, and E. C. Zipf, Absolute cross section for the production of $O(^5S°)$ by electron impact dissociation of O_2, Chem. Phys. Lett., 12 (2), 1971, 288–290.

[4]. R. Celiberto, U. T. Lamanna, and M. Capitelli, Dependence of electron-impact dissociative excitation cross sections on the initial vibrational quantum number in H_2 and D_2 molecules: $X\ ^1\Sigma_g^+ \rightarrow B\ ^1\Sigma_u^+$ and $X\ ^1\Sigma_g^+ \rightarrow C\ ^1\Pi_u$ transitions, Phys. Rev. A, 50 (6), 1994, 4778–4785.

[5]. Yu. M. Smirnov, Dissociative excitation of the HI Balmer series spectral lines in collisions of electrons with H_2 and H_2O mollecules, High Energy Chemistry, 24 (3), 1990, 233–235.

[6]. Yu. M. Smirnov, Cross-sections for dissociative excitation of the OII quartet states by electron impact, Journal of Applied Spectroscopy, 51 (5), 1989, 1132–1135.

[7]. Yu. M. Smirnov, Cross-sections for dissociative excitation of the NI doublet states,Optics and Spectroscopy, 61 (1), 1986, 33–38.

[8]. Yu. M. Smirnov, Investigation of inelastic collisions of slow electrons with tellurium molecules, High Energy Chemistry, 26 (2), 1992, 99–103.

[9]. Yu. M. Smirnov, Formation of excited singly charged selenium ions by e-Se_2 collisions, Optics and Spectroscopy, 100 (5), 2006, 667–674.

[10]. A. N. Kuchenev and Yu. M. Smirnov, Effective cross-sections for inelastic collisions of slow electrons with yttrium monooxyde molecules, High Energy Chemistry, 25 (3), 1991, 202–207.

[11]. Yu. M. Smirnov, Dissociative excitation of K and K^+ emission by electron impact on KI molecules, Chem. Phys., 192 (3), 1995, 379–385.

[12]. Yu. M. Smirnov, Dissociative excitation of odd quintet levels of iron atom by electron collisions with iron dichloride molecules, Russian Journal of Physical Chemistry B, 4 (3), 2010, 379–383.

[13]. Yu. M. Smirnov, Dissociative excitation of odd doublet levels of cobalt atom by electron collisions with cobalt dichloride molecules, Russian Journal of Physical Chemistry B, 5 (2), 2011, 188–196.

[14]. Yu. M. Smirnov, Excitation of gallium one-charged ion in e-Ga collisions, J. Phys. B:At. Mol. Opt. Phys., 48 (16), 2015, 165204.

[15]. Yu. M. Smirnov, TlII excitation cross-sections in collisions of slow electrons with thallium atoms, J. Phys. B:At. Mol. Opt. Phys., 49 (17), 2016, 175204.

[16]. Yu. M. Smirnov, Dissociative excitation of even doublet levels of cobalt atom by e-$CoCl_2$ collisions, High Energy Chemistry, 37 (2), 2003, 55–59.

[17]. J. C. Pickering and A. P. Thorne, The spectrum and term analysis of CoI, Astrophys. J. Suppl. Ser., 107 (1996) 761–809.
[18]. K. P. Huber and G. Herzberg, Molecular Spectra and Molecular Structure. IV. Constants of Diatomic Molecules (New York, Cincinnati, Atlanta et al: Van Nostrand Reinhold Company, 1979).
[19]. Yu. M. Smirnov, Dissociative excitation of singlet levels of nickel atom by e-$NiCl_2$ collisions, Khimicheskaya Fizika (Chemical Physics), 20 (9), 2001, 14–19.
[20]. Yu. M. Smirnov, Excitation cross-sections of the $^4D°$ levels of cobalt atom by electron impact, Journal of Applied Spectroscopy, 64 (5), 1997, 573–577.
[21]. Yu. M. Smirnov, Excitation cross-sections of the $^4F°$ levels of cobalt atom by electron impact, High Temperature, 36 (2), 1998, 163–168.

*Smirnov Yu.M. "Dissociative Excitation of the odd Quartet Levels of Cobalt Atom in e–CoCl2 Collisions." International Journal of Research in Engineering and Science (IJRES), vol. 05, no. 10, 2017, pp. 41–49.